ANGULAR DEPENDENCE OF M X-RAY PRODUCTION DIFFERENTIAL CROSS-SECTIONS AT 5.96 keV

R. Durak, Y. Özdemir, A. Ateş, M. Sağlam, S. Erzeneoğlu and M. Biber
Department of Physics, Faculty of Science&Arts, Atatürk University, 25240 Erzurum, TURKEY

ABSTRACT

The knowledge of the angular dependence of *M* shell production differential cross-sections is important because of their extensive use in basic studies of photoelectric effect, characteristic X-ray production, internal conversion of γ-rays, radiative and non-radiative transition probabilities and development of more reliable angular dependence theoretical models describing fundamental inner-shell ionization processes. The angular dependence of M X-ray production differential cross-sections for selected heavy elements between Lu and Pt have been measured at 5.59 keV incident photon energy, at seven emission angles in the range 120° - 150° at intervals of 5°. The emission angle was set to 0°. The target M X-ray spectra were recorded by the collimated Si(Li) detector, which has an active area of 12.5 mm^2, a sensitive crystal depth of 3 mm and a Be window of 0.025 mm thickness. The measured energy resolution of the detector system was 188 eV for an amplifier shaping time constant of 6 μs at the 5.9 keV peak of 55Fe. Angular dependence M X-ray production differential cross-sections have been derived, using the M-shell fluorescence yields, experimental total M X-ray production cross-sections and theoretical M-shell photoionization cross-sections. M X-ray production differential cross-sections are found to decrease with increase in the emission angle, showing an anisotropic spatial distribution of M X-rays. To the best of our knowledge, no other experimental results are available for worked elements in the angular range 120°-150° for comparison with present results. Extracted results have been compared with the theoretical predictions and semi empirical fits. The present experimental results are in good agreement with the theoretical values.

1. INTRODUCTION

The knowledge of the angular dependence *M*-shell production differential cross-sections are important because of their extensive use in basic studies of photoelectric effect, characteristic X-ray production, internal conversion of γ-rays, radiative and non-radiative transition probabilities and developing more reliable angular dependence theoretical models describing fundamental inner-shell ionization processes. Experimental and theoretical several attempts have been made for *K* and *L* X-ray angular correlation (1-12).

Previous investigators (13-16) have reported that subsequent to photoionization of *K* and *L* shell electrons, the emission of the $K\alpha$, $K\beta$, $L\beta$ and $L\gamma$ groups of fluorescence X-ray lines is isotropic while that of $L\ell$ and $L\alpha$ groups is anisotropic in spatial distribution. It was concluded that the L_3 vacancy states with $J = 3/2$ are aligned whereas the L_1 and L_2 vacancy states with $J = 1/2$ are non-aligned. According to Cooper and Zare (17), the spatial distribution of X-ray emission for different magnetic substances is always isotropic; but in the theoretical calculations by Papp *et al.* (18), it is shown that the spatial distribution of X-rays is different for different magnetic subshell. Furthermore, the calculations of Cooper and Zare (17) predict that after photoionisation the inner-shell vacancy state has equal population of magnetic substates and is therefore not alignment. Extensive literature search reveals that the angular dependence *M* X-ray production differential cross-sections for the elements Lu, Hf, Ta, W, Os and Pt, especially for the angular range 120° - 150° are not available, due to the complexity associated with the M X-ray spectrum and experimental difficulties.

In view of the above status, we felt necessary to investigate angular dependence of the *M* X-ray production differential cross-sections. In the present study, we have measured angular dependence of the *M* X-ray production differential cross-sections for heavy elements Lu, Hf, Ta, W, Os and Pt at 5.96 keV of indicent photon energy using a fluorescence excitations technique. The experimental geometry, the method of measurement and experimental results have been reported in this paper.

2. EXPERIMENTAL DETAILS

The experimental arrangement and geometry used in the present study are shown in Figure 1. The source-target geometry was varied at different angles varying from 120° to 150° at intervals of 5°. The emission angle was set to 0°. The target *M* X-ray spectra were recorded by the collimated Si(Li) detector having an active area of 12.5

mm^2, a sensitive crystal depth of 3 mm and a Be window of 0.025 mm thickness. The measured energy resolution of the detector system was 188 eV for an amplifier shaping time constant of 6 μs at the 5.9 keV peak of ^{55}Fe. The detector was placed in a lead-housing to minimize detection of radiations directly from the source and those scattered from the surroundings. Spectroscopically pure targets of 1.70 cm^2 area and thickness ranging from 3 to 35 mg/cm^2 were used. The spectra were accumulated in time intervals ranging from 43200 s to 280800 s in order to obtain sufficient statistical accuracy and detection limits for low probability events. The *M* X-rays photo peak areas were evaluated by fitting of multi-Gaussian function plus polynomial background.

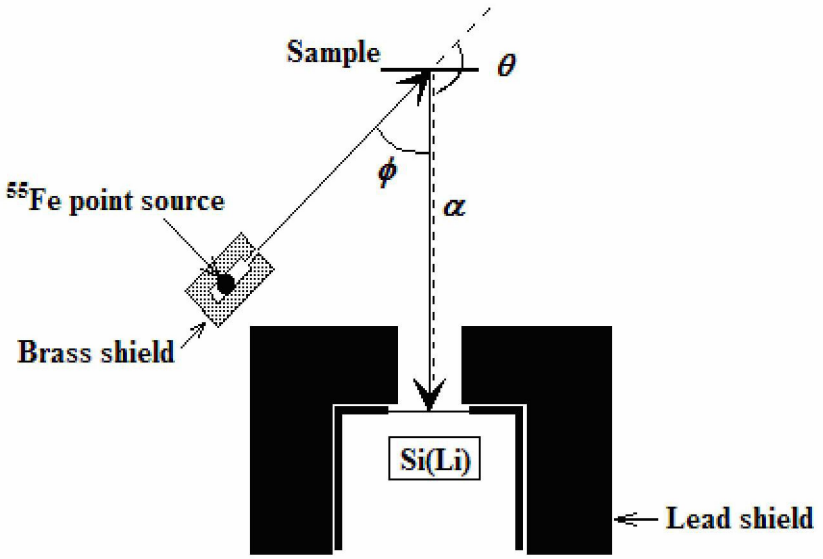


Figure 1. Experimental set-up used for measurements of angular dependence M X-ray production cross-section.

3. DATA ANALYSIS

Experimental method

The experimental values of angular dependence *M* X-ray production differential cross-sections for heavy elements were given by

$$\frac{d\sigma_M^\theta}{d\Omega} = \frac{N_M^\theta}{4\pi (I_0 G)^\theta \varepsilon_M^\theta \beta_M^\theta t} \tag{1}$$

where N_M^θ (θ = 120°-150°) are the net counts per unit time under the *M* X-ray peak, $(I_0 G)^\theta$ is the intensity of exciting radiation falling on the portion of sample visible to the detector, ε_M^θ is the detector efficiency for the *M* X-rays of the element, t is the mass per unit area of the element (g cm^{-2}) and β_M^θ the absorption-correction factor that accounts for absorption of the incident photons and emitted *M* X-rays in the target is the self absorption correction factor of the target material and is given by:

$$\beta_M^\theta = \frac{1 - \exp[-(\mu_i \sec\phi + \mu_e \sec\alpha)t]}{(\mu_i \sec\phi + \mu_e \sec\alpha\ )t} \tag{2}$$

Where μ_i and μ_e are the total mass absorption coefficients of target material at the incident photon and emitted *M* X-rays energies, respectively (19). t is the thickness of the sample. ϕ and α are the angles of the incident and emitted X-ray with respect to the target normal, ϕ and α were set to 30°-60° and 0, respectively in present

set-up. In this study, the values of $(I_0 G\varepsilon_M)^\theta$ were determined by collecting the K X-ray yields from thin standard samples of Al, Si, P, S, Cl, K, Ca and Ti using the relation:

$$(I_0 G\varepsilon_K)^\theta = \frac{N_K^\theta}{\sigma_K^x(E)\beta_K^\theta t} \tag{3}$$

Where N_K^θ, β_K^θ and ε_K are as in Equation 1. But for K instead of M X-rays. σ_K^x values were derived:

$$\sigma_K^x = \sigma_K^p(E)\omega_K \tag{4}$$

Where $\sigma_K^p(E)$ is the K shell photoionization cross-section for the element at excitation energy E from tables of Scofield (20) and ω_K is K shell fluorescence yields from tables of Hubbell (21). The measured $(I_0 G\varepsilon_K)^\theta$ $(\theta = 120^0)$ values for the present set-up are plotted as a function of energy in Figure 2.

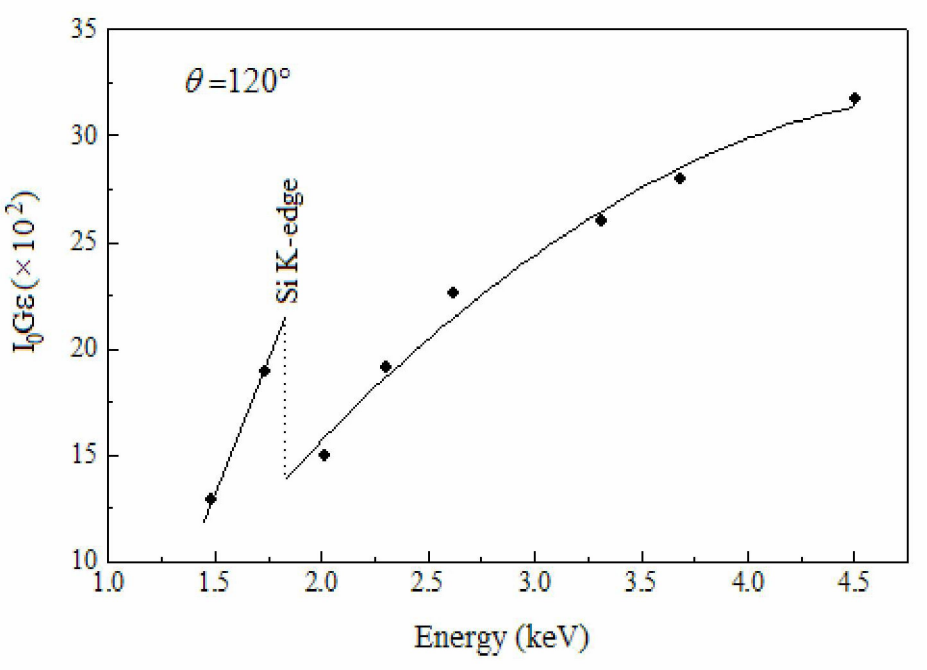


Figure 2. Plot of the factor $I_0 G\varepsilon$ $(\theta = 120^0)$ vs. K X-ray energy.

Theoretical model

The theoretical M X-ray production differential cross-sections values for heavy elements were deduced from the relation:

$$\frac{d\sigma_M}{d\Omega} = \frac{\sigma_M^p(E)\varpi_M}{4\pi} \tag{5}$$

where $\sigma_M^p(E)$ is the M shell photoionization cross-section for the element at excitation energy E from tables of Scofield (20) and ϖ_M is M shell fluorescence yields from tables of Hubbell (21).

4. RESULTS AND DISCUSSION

The present measured M X-rays production differential cross-sections in Lu, Hf, Ta, W, Os and Pt at 5.96 keV of indicent photon energy in the angular range 120°-150° are listed in Table 1 and compared with the available theoretical predictions and fitted values. The experimental results for Lu ve W are represented grafically as M X-

rays production differential cross-sections vs. $\cos\theta$ (θ =120°-150°) in Figures 3 a,b. It has been observed that *M* X-ray production differential cross-sections decrease with increase in the emission angle. Present experimental values were fitted to a second-order polynomial as a function of $\cos\theta$ ($= \sum_n A_n Z^n$) and fitted values in the same table. The fitted coefficients are listed in Table 2. Using our fitted values, the experimental angular dependence *M* X-rays production differential cross-sections for all elements in the range $71 \le Z \le 78$ can be obtained for comparison and the fit will be valid in the seven angles from 120° to 150°.

The overall error in the measured angular dependence *M* X-ray production differential cross-sections are estimated to be less than 1.5 % - 2.8 %, which arises due to the uncertainties in the various physical parameters required to evaluate the experimental results using Equation 1. It is evident from Table 1 and Figure 3 that the present experimental results are in good agreement with the theoretical values.

The angular dependence *M* X-ray production differential cross-sections are found to decrease with increase in the emission angle, showing anisotropic spatial distribution. To the best of our knowledge, no other experimental results are available for worked elements in the angular range 120°-150° for comparison with present results. Therefore, the results obtained in the present study constitute the first experimental measurements.

Consequently, much more experimental information will need to be available before a meaningful comparison of experiment and theory becomes possible.

Table 1. Comparison of present experimental, theoretical and fitted *M* X-ray production differential cross-sections ($cm^2/g\ sr$).

	Lu				Hf				Ta		
θ(°)	Experimental	Fitted	Theo.		Experimental	Fitted	Theo.		Experimental	Fitted	Theo.
120°	0.298±0.006	0.299			0.341±0.005	0.337			0.349±0.006	0.350	
125°	0.295±0.006	0.294			0.339±0.005	0.329			0.345±0.006	0.343	
130°	0.291±0.006	0.288			0.328±0.006	0.321			0.338±0.006	0.335	
135°	0.279±0.006	0.281	0.293		0.315±0.005	0.312	0.325		0.325±0.005	0.338	0.362
140°	0.270±0.005	0.274			0.317±0.005	0.303			0.321±0.005	0.322	
145°	0.271±0.005	0.268			0.300±0.005	0.295			0.319±0.005	0.317	
150°	0.262±0.005	0.262			0.298±0.005	0.286			0.311±0.005	0.311	
	W				Os				Pt		
θ(°)	Experimental	Fitted	Theo.		Experimental	Fitted	Theo.		Experimental	Fitted	Theo.
120°	0.403±0.009	0.406			0.480±0.012	0.479			0.599±0.013	0.600	
125°	0.398±0.008	0.392			0.464±0.013	0.468			0.590±0.013	0.589	
130°	0.376±0.009	0.377			0.461±0.011	0.456			0.580±0.012	0.578	
135°	0.358±0.008	0.360	0.401		0.440±0.012	0.444	0.487		0.564±0.012	0.565	0.595
140°	0.345±0.008	0.345			0.431±0.010	0.433			0.554±0.012	0.553	
145°	0.331±0.007	0.332			0.431±0.009	0.423			0.540±0.010	0.542	
150°	0.320±0.009	0.318			0.410±0.008	0.413			0.531±0.010	0.530	

Table 2. Angular dependence M X-ray production cross-sections fitted to the $\sum_n A_n Z^n$ as a function of cosθ (θ=120°-150°).

	Fitting coefficient		
Elements	A_0	A_1	A_2
Lu	0.31498	-0.00911	-0.08070
Hf	0.36150	-0.01271	-0.10098
Ta	0.40039	0.09689	-0.00623
W	0.47394	0.07704	-0.11696
Os	0.53632	0.08100	-0.06891
Pt	0.62229	-0.03649	-0.16409

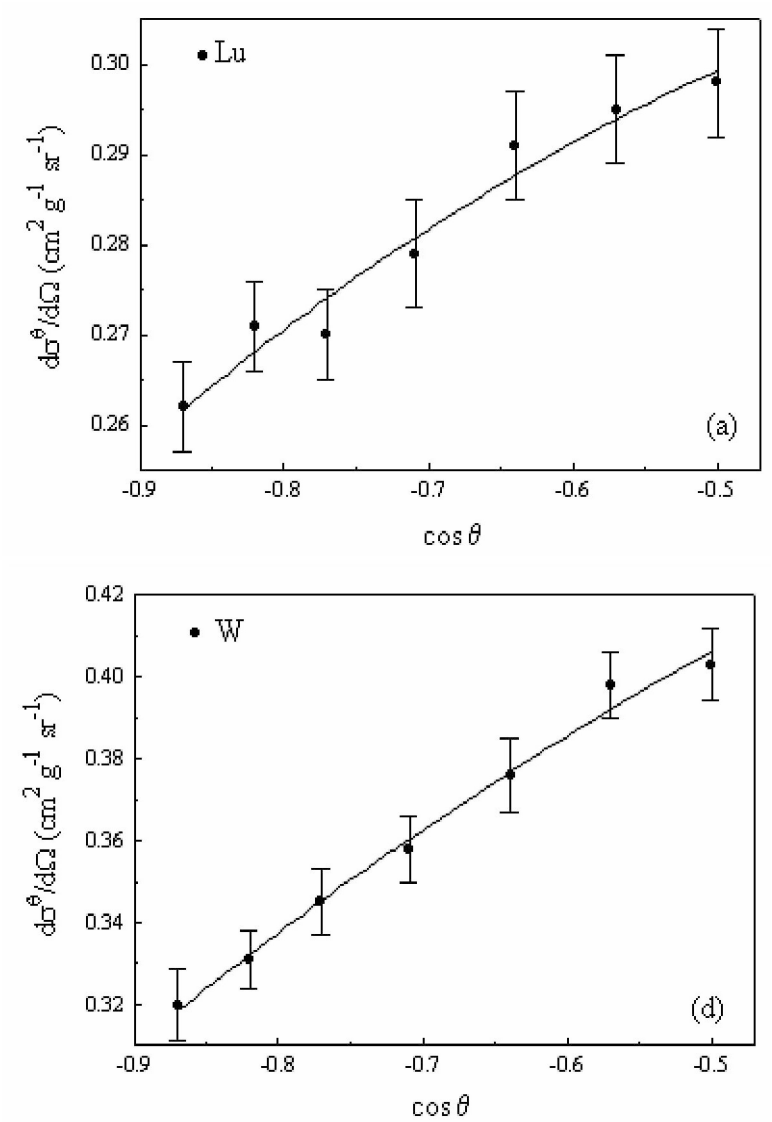


Figure 3. The measured values of the angular dependence *M* X-rays production differential cross-sections are plotted as a function of $\cos\theta$ for Lu and W.

5. REFERENCES

1. R. Anholt, J.O. Rasmussen, *Phys. Rev. A*, 9, 585 (1974).
2. A.L. Catz, *Phys.Rev. A*, 3, 849 (1970).
3. A.L. Catz, E.S. Macias, *Phys. Rev. A*, 3, 849 (1971).
4. M. Ertuğrul, E. Büyükkasap, A. Küçükönder, A.İ. Kopya, H. Erdoğan, *Nuova Cimento*, 17, 993 (1995).
5. M.R. Zalutsty, E.S. Macias, *Phys. Lett. A,* 49, 285 (1974).
6. J.H. Scofield, *Phys. Rev. A*, 40, 3054 (1989).
7. J.H. Scofield, *Phys. Rev. A.*, 14, 1418 (1976).
8. J.W. Cooper, R.N. Zare, *J. Chem. Phys.*, 48, 942 (1968).
9. K. Bulum, H. Kleinpopen, *Phys. Rep.*, 52, 203 (1979).
10. K. Bulum, H. Kleinpopen, *Phys. Rep.*, 96, 251 (1983).
11. J.W. Cooper, R.N. Zare, *J. Chem. Phys.*, 48, 942 (1968).
12. M. Ertuğrul, R. Durak, E. Tıraşoğlu, E. Büyükkasap, H. Erdoğan, *Appl. Spectrosc. Rev.*, 30 (3), 219 (1995).
13. K.S. Kahlon, K. Shatentra, K.L. Allawadhi, B.S. Sood, *Pramana-J. Phys.*, 35, 105 (1990).
14. K.S. Kahlon, H. Aulakh, S. Singh, N.R. Mittal, K.L. Allawadhi, B.S. Sood, *Phys. Rev. A* 43, 1455 (1991).
15. K.S. Kahlon, H. Aulakh, S. Singh, N.R. Mittal, K.L. Allawadhi, B.S. Sood, *Phys. Rev. A*, 44, 4379 (1991).
16. K.S. Kahlon, K.L. Allawadhi, B.S. Sood, *J. Phys. B: At. Mol. Opt. Phys.*, 32 (15), 3701 (1991).
17. J.W. Cooper, R.N. Zare, ''Atomic Collisions Processes'', Vol. XIC. Gordon and Breach, New York 1969, p.317.
18. T. Papp, J. Polinkas, L. Sarkadi, *Phys. Rev. A*, 42, 5452 (1990).
19. J.H. Hubbell, S.M. Seltzer, National Institute of Standards and Technology Report No. NISTIR 5632, (1995).
20. J.H. Scofield, Lawrence Livermore National Report No. UCRL 51326, (1973).
21. J.H. Hubbell, P.N. Trehan, N. Singh, B. Chand, D. Mehta, M.L. Garg, R.R. Garg, S. Singh, S. Puri, *J. Phys. Chem. Ref. Data* 23, 339 (1994).